

ARTICLE

Elastic Tensor and Thermodynamic Property of Magnesium Silicate Perovskite from First-principles Calculations

Zi-jiang Liu^{a,b*}, Xiao-wei Sun^b, Cai-rong Zhang^c, Jian-bo Hu^d, Ting Song^b, Jian-hong Qi^a

a. Department of Physics, Lanzhou City University, Lanzhou 730070, China

b. School of Mathematics and Physics, Lanzhou Jiaotong University, Lanzhou 730070, China

c. Department of Applied Physics, Lanzhou University of Technology, Lanzhou 730050, China

d. Materials and Structures Laboratory, Tokyo Institute of Technology, Yokohama 226-8503, Japan

(Dated: Received on June 25, 2011; Accepted on August 19, 2011)

The thermodynamic and elastic properties of magnesium silicate (MgSiO_3) perovskite at high pressure are investigated with the quasi-harmonic Debye model and the first-principles method based on the density functional theory. The obtained equation of state is consistent with the available experimental data. The heat capacity and the thermal expansion coefficient agree with the observed values and other calculations at high pressures and temperatures. The elastic constants are calculated using the finite strain method. A complete elastic tensor of MgSiO_3 perovskite is determined in the wide pressure range. The geologically important quantities: Young's modulus, Poisson's ratio, Debye temperature, and crystal anisotropy, are derived from the calculated data.

Key words: Thermodynamic property, Elastic property, MgSiO_3 perovskite

I. INTRODUCTION

The lower mantle plays a critical role in understanding the evolution of the Earth. Compositional models for the lower mantle have thus been extensively examined, by comparing seismological models with calculated densities and seismic velocities of mixtures of plausible constituents [1–4]. Due to magnesium silicate (MgSiO_3) perovskite (orthorhombic structure, space group $Pbnm$) is believed to be the most abundant constituent in the lower mantle with more than 75% in volume, the validity of such models strongly depends on knowledge of the elastic properties of high-pressure phases MgSiO_3 perovskite. The experimental determination of elastic properties at extreme conditions is, however, not an easy task. Elastic constants have been studied experimentally only under ambient conditions [5]. Therefore, another approach has been developed based on first-principles quantum mechanical theory. First-principles calculations provide the ideal complement to the laboratory approach. Such calculations have true predictive power and can supply critical information including that which is difficult to be measured experimentally. The previous theoretical calculations studied the elastic constants of MgSiO_3 perovskite using the approach [6–11]. However, many of its elastic tensor is still relatively poorly known. Many properties

play crucial role in the interpretation of seismic data, and thus have a large influence on our knowledge of the Earth's interior, such as Young's moduli, Poisson's ratio, shear anisotropy, the anisotropy of linear bulk modulus, and the anisotropy of every symmetry plane and axis *etc.*

Accurate determination of the thermal properties of MgSiO_3 perovskite is of particular geophysical interest because it can be used to directly constrain the compositional and mineralogical model of the lower mantle by comparing with the observed seismic data. It is surprising that MgSiO_3 perovskite has received little attention on its thermodynamic properties under high temperature and high pressure. For example, its equation of state (EOS) is relatively well known only at 298 K [12, 13], the thermal expansion, α , the reported values under ambient conditions are scattered between 1.7 and 2.2 [1, 14–16].

Oganov *et al.* used high-temperature *ab initio* molecular dynamic simulations to study the equation of state of MgSiO_3 perovskite under lower mantle pressure-temperature conditions [7]. Karki *et al.* applied a first-principles approach based on density-functional perturbation theory to determine the pressure dependence of phonon dispersion for MgSiO_3 perovskite to 150 GPa and to derive several thermodynamic quantities of interest [17]. A study of MgSiO_3 perovskite shows that this material can be considered as a Debye-like solid [18], *i.e.*, the Debye model gives an acceptable description of the phonon contribution to the total free energy. In order to further understand the thermodynamics of MgSiO_3 perovskite, in the present work we use the

* Author to whom correspondence should be addressed.
E-mail: liuzj2000@126.com, Tel.: +86-931-7601256, FAX: +86-931-7601142

TABLE I Structure and elasticity of MgSiO₃ perovskite at $P=0$ GPa^a.

	GGA	HF [25]	LDA [26]	LDA [8]	LDA [11]	GGA [75]	Exp. [5]
$a_0/\text{\AA}$	4.7943	4.786	4.711	4.7891		4.8337	4.7747
$b_0/\text{\AA}$	4.9241	4.913	4.880	4.9219		4.9830	4.9319
$c_0/\text{\AA}$	6.8992	6.896	6.851	6.8925		6.9767	6.8987
$V_0/\text{\AA}^3$	162.88	162.12	157.50	162.47	164.1	168.04	162.45
B_0/GPa	241						
B'_0	4						
c_{11}	462		496	499	449	444	482
c_{22}	518		560	561	500	489	537
c_{33}	419		504	466	434	408	485
c_{44}	202		151	217	183	194	204
c_{55}	177		198	186	162	172	186
c_{66}	130		171	160	138	131	147
c_{12}	107		132	123	123	110	144
c_{13}	136		136	137	129	126	147
c_{23}	147		156	142	144	136	204
B/GPa	242	309	267.1	258.3	241	231.3	264
G/GPa	167		178.7	186.3	161	162.3	177.4
B/G	1.449						
E/GPa	407						
σ	0.219						
$\nu_l/(\text{km/s})$	10.648		10.926	10.953	10.60	10.62	11.042
ν_t	6.383		6.498	6.641	6.30	6.395	6.574
θ_D/K	1045		1077	1097		1036	1078

^a a_0 , b_0 , and c_0 are the equilibrium lattice parameters, V_0 is the equilibrium volume, B_0 is the bulk modulus, B'_0 is pressure derivative at zero pressure, c_{ij} is the elastic constant, B is the adiabatic bulk moduli, G is the shear modulus, B/G is an indication of ductile *vs.* brittle characters, E is the Young modulus, σ is the Poisson's ratio, ν_l and ν_t are the longitudinal and transverse elastic waves of polycrystalline material, θ_D is the Debye temperature.

quasi-harmonic approximation with the Debye model combined with the first principle calculations to study the thermodynamic properties of MgSiO₃ perovskite at high temperature and high pressure [19].

We also apply the pseudopotentials plane-wave method within the generalized gradient approximation (GGA) in the framework of the density functional theory (DFT) to the study of the elastic properties of MgSiO₃ perovskite. Based on *ab initio* study and the quasi-harmonic Debye model, the thermodynamic properties including the heat capacity, the thermal expansion, the bulk modulus and its first pressure derivative are obtained in detail.

II. COMPUTATIONAL METHOD

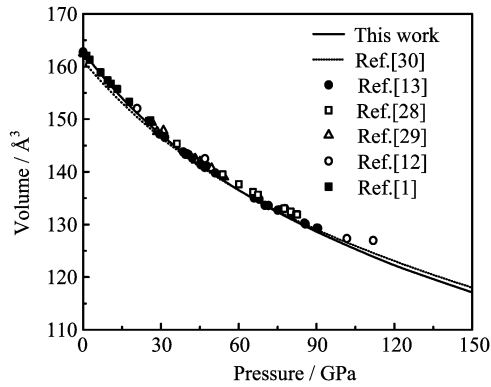
The first-principles calculations are performed by employing pseudopotential plane-waves approach based on DFT [20, 21] and implemented using the Cambridge serial total energy package (CASTEP) code [22]. The exchange-correlation potential is calculated by the GGA based on Perdew *et al.* [23]. In order to reduce the number of plane-waves required, chemically inac-

tive core electron are effectively replaced with ultrasoft pseudopotential, which in this work are taken from the CASTEP database. Two parameters that affect the accuracy of calculations are the kinetic energy cutoff, which determines the number of plane-waves in the expansion, and the number of special k points used for the Brillouin zone integration. A plane wave basis set is used with 380 eV cutoff. The k integrations over the Brillouin zone are performed up to $5 \times 5 \times 4$ Monkhorst-Pack mesh [24]. The self-consistent calculations are considered to be converged when the total energy of the system is stable within 5 $\mu\text{eV}/\text{atom}$.

III. RESULTS AND DISCUSSION

A. Structural property

The calculated structural properties of MgSiO₃ perovskite using the pseudopotential plane-waves method are summarized in Table I, along with the available experimental data [5] and other theoretical results [7, 8, 11, 25, 26]. It can be seen that the calculated equilibrium volume is close to the experimental result [5], and

FIG. 1 Equation of state of MgSiO₃ perovskite.

is in good agreement with the theoretical result [8]. The calculated unit cell volumes at fixed values of applied hydrostatic pressure from 0 GPa to 150 GPa are used to construct the EOS, which is fitted to a third order Birch-Murnaghan equation [27]. We obtain, by least-squares fitting, the bulk modulus B_0 and its pressure derivative B'_0 at zero pressure. These are listed in Table I. From Table I we can see that the calculated value of B_0 from the elastic constants has nearly the same value as the one obtained from the EOS fitting. The pressure-volume relation obtained in the present study is compared with those from experimental [1, 12, 13, 28, 29] and first-principles studies [30] in Fig.1. The excellent agreement strongly supports the choice of pseudopotentials and the GGA approximation for the present study.

B. Thermodynamic property

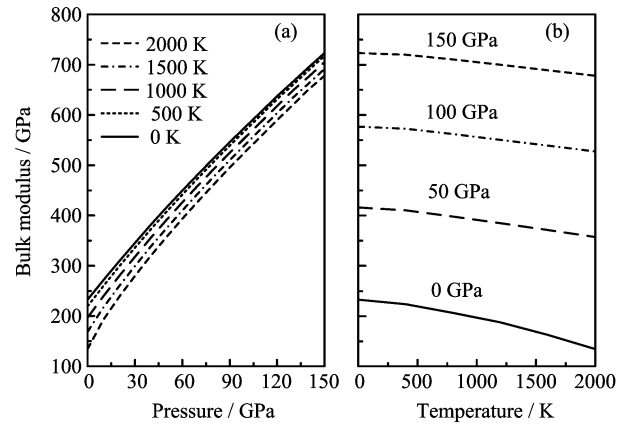
The correct temperature variation of the thermodynamic properties can only be obtained by treating the lattice vibrations as quantized (phonons). The thermal effects in this study are investigated within the quasi-harmonic Debye theory of crystals [31], without having to make extensive and complicated lattice dynamic calculations.

The approximation is used to determine the Debye temperature given as

$$\Theta = \frac{\hbar}{k_B} (6\pi^2 V^{1/2} n)^{1/3} f(\sigma) \sqrt{\frac{B_S}{M}} \quad (1)$$

where V , M , n , B_S , $f(\sigma)$, and k_B are the molar volume, the molar mass, the number of atoms per formula unit, the adiabatic bulk moduli, a scaling function that depend on Poisson's ratio of the solid, and the Boltzmann constant, respectively. A simple way to use the Debye model is to consider that the adiabatic bulk modulus is equal to the isothermal bulk modulus B_T leading to:

$$B_S \approx B(V) = V \left[\frac{d^2 E(V)}{dV^2} \right] \quad (2)$$

FIG. 2 Pressure (a) and temperature (b) dependence of the bulk modulus of MgSiO₃ perovskite.

where E is the total energy of the crystal at 0 K. Given the energy of the considered phase as a function of the molecular volume by means of the plane-waves method at static condition, the quasi-harmonic Debye model allows to (i) to generate the Debye temperature $\Theta(V)$ from Eqs. (1) and (2), (ii) to obtain the non-equilibrium Gibbs function $G^*(V; P, T)$:

$$G^*(V; P, T) = E(V) + PV + A_{\text{vib}}(\Theta(V); T) \quad (3)$$

where A_{vib} is the vibrational Helmholtz free energy given by the Debye model, and (iii) to minimize G^* to derive the thermal equation of state $V(P, T)$ and the chemical potential $G(P, T)$ of the corresponding phase. The standard thermodynamic relations that depend on temperature and pressure are used to derive other macroscopic properties. A detailed description of this procedure can be found in Ref.[31].

Through the quasi-harmonic Debye model, one can calculate the thermodynamic quantities of MgSiO₃ perovskite at any temperature and pressure. In the present work, the thermal properties are determined in the temperature range from 0 K to 2000 K, and the pressure effect is studied in the range of 0–150 GPa. We calculate the dependence of the isothermal bulk modulus on pressure and temperature, as shown in Fig.2. It is found that the bulk modulus of MgSiO₃ perovskite increases linearly with pressure at constant temperature. Considering the change of the equilibrium unit cell volume with pressure, it can be concluded that the dramatic volume variation results in a rapid decrease in the isothermal bulk modulus. The isothermal bulk modulus increases with pressure at given temperature and decreases with temperature at given pressure. These results are due to the fact that the effect of increasing the pressure on the material is the same as decreasing the temperature of the material. The pressure derivatives of the isothermal bulk modulus at given temperature and pressure are very important for the high-pressure studies [32, 33]. From a geophysical viewpoint, the first pressure derivative $B'_{T,P}$ of isothermal bulk modulus is a parameter

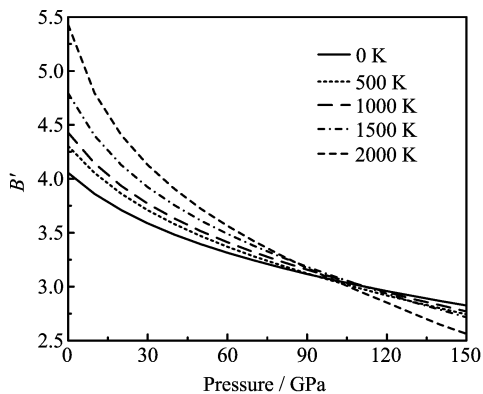


FIG. 3 The predicted first pressure derivative of isothermal B_0 of MgSiO_3 perovskite versus pressure at different temperature.

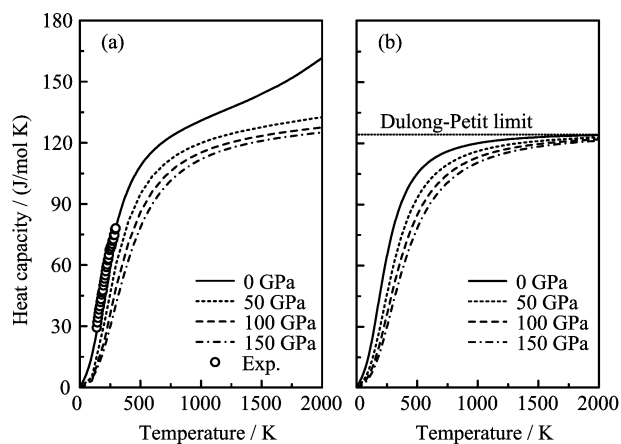


FIG. 4 Temperature dependence of the constant pressure heat capacity (a) and the constant volume heat capacity (b) of MgSiO_3 perovskite.

that is necessary for the accurate inversion of seismic data into composition, structure, and texture, as well as for determining the thermal profile of the deep Earth and also for determining the isothermal empirical equation of the state of materials in the deep Earth [34].

Figure 3 shows the predicted first pressure derivative of the isothermal B_0 of MgSiO_3 perovskite versus pressure at different temperatures. It can be seen that the B' increases with the increase of temperature when $P < 105$ GPa and decreases with the increase of temperature when $P > 105$ GPa.

The knowledge of the heat capacity of a crystal not only provides essential information on its vibrational properties but also is mandatory for many applications. To further confirm the validity of our calculations, the comparison of the heat capacity at constant pressure (C_P) between the calculation and the experiment is presented in Fig.4(a). It shows that the calculated values are in good agreement with the experimental values [35]. Figure 4 shows the difference between the heat capacity at constant volume (C_V) and C_P is small at low tem-

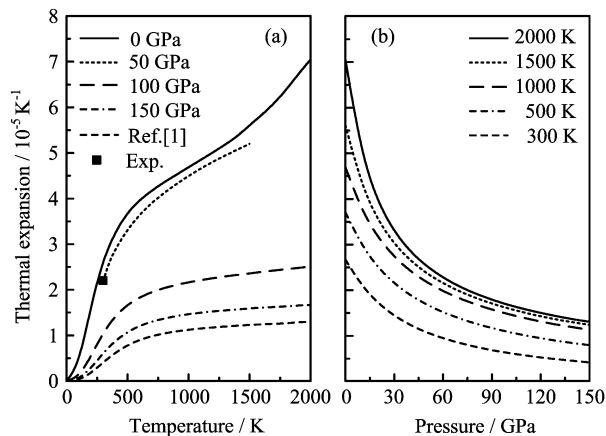


FIG. 5 Temperature (a) and pressure (b) dependence of the thermal expansion coefficient of MgSiO_3 perovskite.

peratures and both of them follow the relationship of the Debye model ($C(T) \propto T^3$). At high temperatures, C_V converges to a near-constant value (Dulong-Petit limit) while C_P increases monotonously with the temperature. Figure 4 also indicates that temperature and pressure have opposite influences on the heat capacity and the effect of temperature on the heat capacity is more significant than that of pressure.

The thermal expansion coefficient α dependence on pressure and temperature is presented in Fig.5. The calculated α is in accordance with the available measured value [36] at ambient conditions and the fitted values [1] at zero pressure. It is shown that, for a given pressure, α increases with temperature at low temperature especially at 0 GPa and gradually tends to a linear increase at high temperature. With increasing pressure, the increase in α with temperature becomes smaller. For a given temperature, α decreases strongly with increasing pressure and remains very small at high temperatures and high pressures. This is mainly because the anharmonic effect becomes less important at high pressures. With the increase of pressure, the volume of the solid reduces and the atoms come closer to each other, increasing the depth of the potential energy well and reducing the anharmonic nature of the potential energy curve at high temperatures. Since thermal expansivity is a result of anharmonicity in the potential energy, it becomes virtually independent of pressure and temperature in the high pressure and temperature domain [37].

C. Elastic property

Several methods are available for computation of stiffness coefficients but the finite strain method is the most commonly used one. In this approach, the ground state structure is strained according to symmetry dependent strain patterns with varying amplitudes and the stress tensor is determined after a re-optimization of the in-

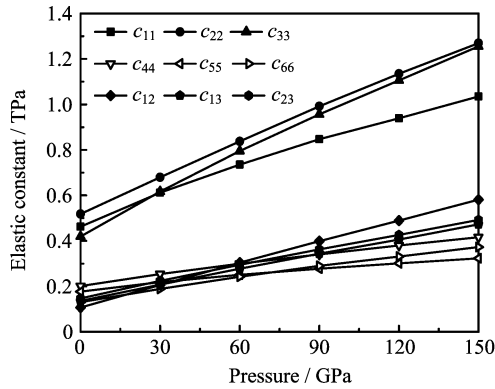


FIG. 6 Pressure dependence of elastic constants of MgSiO₃ perovskite.

ternal structure parameters. The elastic stiffness coefficients are then the proportionality coefficients relating the applied strain to the computed stress, $\sigma_i = c_{ij}\varepsilon_j$ [38, 39]. In order to avoid the plastic deformation, the applied perturbed strain must be small. A necessary condition for a crystal to be mechanically stable is that the elastic energy must be positive, or alternatively, its elastic stiffness matrix should satisfy the well-known Born stability criteria [40]. For the orthorhombic crystals, the criteria result in the following conditions:

$$\begin{aligned} c_{11} + c_{22} - 2c_{12} > 0, \quad c_{11} + c_{33} - 2c_{13} > 0, \\ c_{22} + c_{33} - 2c_{23} > 0, \quad c_{11} > 0, \quad c_{22} > 0, \\ c_{33} > 0, \quad c_{44} > 0, \quad c_{55} > 0, \quad c_{66} > 0, \\ c_{11} + c_{22} + c_{33} + 2c_{12} + 2c_{13} + 2c_{23} > 0 \end{aligned} \quad (4)$$

The calculated elastic constants at zero pressure are tabulated in Table I, where we include the available experimental result [5] and other theoretical results [7, 8, 11, 25, 26]. It shows that MgSiO₃ perovskite is mechanically stable. We find at zero pressure $c_{22} > c_{11} > c_{33}$, whereas Brillouin scattering data [5] show $c_{22} > c_{33} > c_{11}$ as previous pseudopotential results do [26]. However, our results are consistent with static compression data [1] and other theoretical data [7, 8, 11], which find that the c axis is most compressible and the b axis least compressible. Because the single-crystal elastic constants of MgSiO₃ perovskite have not yet been measured in experiments at high pressure, the present work predicts the high pressure elastic constants. Figure 6 shows the elastic constants increase smoothly and monotonically with increasing pressure. Above 27 GPa, we find $c_{22} > c_{33} > c_{11}$ indicating that the a axis is the most compressible at higher pressures.

Base on the scheme of Voigt and Reuss and with the approximation of Hill's arithmetic average [41–43], we calculate B and shear modulus G of MgSiO₃ perovskite, shown in Table I. The calculated elastic moduli slightly underestimate the experimental result [5] which are in excellent agreement with the recent first-principles studies [11] and another experimental value

(246 GPa) [44]. Furthermore, the Young modulus E and Poisson's ratio σ are calculated with the following equations for the isotropic material:

$$E = \frac{9BG}{3B + G} \quad (5)$$

$$\sigma = \frac{3B - 2G}{2(3B + G)} \quad (6)$$

The calculated E and σ at zero pressure are also summarized in Table I. σ is associated with the volume change during uniaxial deformation. If $\sigma = 0.5$, no volume change occurs during elastic deformation. The low σ value for MgSiO₃ perovskite means that a large volume change is associated with its deformation. In addition, Poisson's ratio provides more information about the characteristics of the bonding forces than any of the other elastic constants [45]. It has been proven that $\sigma = 0.25$ is the lower limit for central-force solids and 0.5 is the upper limit, which corresponds to infinite elastic anisotropy. The low σ value for MgSiO₃ perovskite indicates that the interatomic forces in the compound are noncentral.

Pugh proposed the ratio of bulk to shear modulus of polycrystalline phases [46], B/G as an indication of ductile *vs.* brittle characters. Indeed one may argue that G represents the resistance to plastic deformation, while B represents the resistance to fracture. A high B/G value indicates tendency for ductility, while a low value indicates a tendency for brittleness. The critical value which separates ductile and brittle materials has been evaluated to be equal to 1.75. The ratio of MgSiO₃ perovskite is less than 1.75. The result suggests that MgSiO₃ perovskite is prone to brittleness.

D. Debye temperature and elastic anisotropy

It is known that as a fundamental parameter, Debye temperature θ_D correlates with many physical properties of solids, such as specific heat, elastic constants, and melting temperature. At low temperatures, the vibrational excitations arise solely from acoustic vibrations. Therefore, θ_D calculated from elastic constants at low temperatures is the same as that determined from specific heat measurements. One of the methods to calculate θ_D is [47]:

$$\theta_D = \frac{hv_m}{k_B} \left(\frac{3n N_A \rho}{4\pi M} \right)^{1/3} \quad (7)$$

where h is Plank's constant, N_A is Avogadro's number, n is the number of atoms in the molecule, ρ is the density, M is the molecular weight. v_m is the average wave velocity which is defined as

$$v_m = \left[\frac{1}{3} \left(\frac{2}{v_t^3} + \frac{1}{v_l^3} \right) \right]^{-1/3} \quad (8)$$

TABLE II The bulk modulus along crystallographic axes a , b , and c , anisotropy in shear elastic factor (A_i , $i=1, 2, 3$), anisotropy in directional bulk modulus (A_{B_a} , A_{B_c}), and anisotropy in compressibility and shear moduli (A_B and A_G in %).

P/GPa	B_a	B_b	B_c	A_1	A_2	A_3	A_{B_a}	A_{B_c}	A_B	A_G
0	693	827	670	1.3233	1.1009	0.6813	0.8378	0.8096	0.1968	1.4347
30	979	1188	1029	1.2479	1.0302	0.8607	0.8241	0.8660	0.1342	0.5136
60	1222	1568	1360	1.2299	0.9637	1.0038	0.7788	0.8669	0.1811	0.3894
90	1435	1967	1660	1.2219	0.9070	1.1145	0.7294	0.8436	0.2555	0.5302
120	1602	2385	1948	1.2319	0.8685	1.2079	0.6715	0.8166	0.3670	0.8282
150	1780	2792	2249	1.2376	0.8401	1.3050	0.6376	0.8056	0.4288	1.1665

TABLE III Anisotropy factors A_+ , A_- for, symmetry plane (ijk) and $[ijk]$ symmetry axis with symmetry plane (ijk) as a function of pressure.

P/GPa	A_-			A_+					
	(010)	(100)	(001)	[100] (010)	[001] (010)	[010] (100)	[001] (100)	[100] (001)	[010] (001)
0	1.1667	1.2677	0.6836	1.0868	1.2520	1.0856	1.4790	0.7347	0.6350
30	1.0729	1.2015	0.8633	1.0794	1.0664	1.1163	1.2935	0.9320	0.7995
60	1.0320	1.1515	1.0088	1.0973	0.9708	1.1054	1.1996	1.1228	0.9076
90	0.9992	1.1143	1.1231	1.1031	0.9061	1.0826	1.1471	1.2944	0.9786
120	0.9857	1.0943	1.2219	1.1305	0.8616	1.0716	1.1176	1.4703	1.0250
150	0.9730	1.0806	1.3233	1.1505	0.8268	1.0709	1.0903	1.6415	1.0830

where v_l and v_t are the longitudinal and transverse elastic waves of polycrystalline material and obtained from Navier's equation as follows [48]:

$$v_l = \sqrt{\frac{3B + 4G}{3\rho}} \quad (9)$$

$$v_t = \sqrt{\frac{G}{\rho}} \quad (10)$$

Since at low temperatures only the acoustic branches of phonons are active, therefore, the estimated Debye temperature from our elastic constants is valid for low temperatures. The calculated Debye temperatures of MgSiO_3 perovskite are presented in Table I. The calculated value of Debye temperature is 1045 K, indicating that MgSiO_3 perovskite is hard with a large wave velocity, and is in good agreement with the experimental value [5] and other theoretical values [7, 8, 26].

The calculation of the elastic anisotropy is well established in the crystal physics. The elastic anisotropy arises from both shear anisotropy and the anisotropy of linear bulk modulus. For the orthorhombic crystal, the shear anisotropic factor for the (100) shear planes between the $\langle 011 \rangle$ and $\langle 010 \rangle$ directions is [49],

$$A_1 = \frac{4c_{44}}{c_{11} + c_{33} - 2c_{13}} \quad (11)$$

For the (010) shear planes between $\langle 101 \rangle$ and $\langle 001 \rangle$ directions it is

$$A_2 = \frac{4c_{55}}{c_{22} + c_{33} - 2c_{23}} \quad (12)$$

and for the (001) shear planes between $\langle 110 \rangle$ and $\langle 010 \rangle$ directions it is

$$A_3 = \frac{4c_{66}}{c_{11} + c_{22} - 2c_{12}} \quad (13)$$

In the case of isotropic crystals, the factors A_1 , A_2 , and A_3 must be one, while any value smaller or greater than unity is a measure of the degree of elastic anisotropy possessed by the crystal. The calculated shear anisotropic factor of MgSiO_3 perovskite are summarized in Table II, we find that the factors A_1 and A_2 decreases with increasing pressure, however, A_3 increases at high pressure.

In order to investigate the contribution of the linear bulk modulus to the elastic anisotropy of MgSiO_3 perovskite, we calculate the bulk modulus along the crystal axes, defined as $B_i = idP/di$, $i=a, b, c$ [49]. The calculated linear bulk modulus along the three directions a, b, c is listed in Table II, it is noted that the linear bulk modulus of the three directions increases with increasing pressure. It shows that the mechanical anisotropy of MgSiO_3 perovskite gradually strengthen with pressure increasing. The compressibility anisotropy of bulk modulus along a and c axes with respect to b axis can then be written as,

$$A_{B_a} = B_a/B_b, \quad A_{B_c} = B_c/B_b \quad (14)$$

For these two parameters, a value of unity represents elastic isotropy and any deviation from one indicates the degree of the elastic anisotropy. The calculated results are reported in Table II.

However, in the cubic crystals, the linear bulk modulus is the same for all directions, and the compressibility anisotropy is not applied. To overcome this limitation, Chung and Buessem introduced a more practical measure of elastic anisotropy called percentage elastic anisotropy [50]. The percentage anisotropy in compressibility and shear are defined as,

$$A_B = \frac{B_V - B_R}{B_V + B_R}, \quad A_G = \frac{G_V - G_R}{G_V + G_R} \quad (15)$$

For the percentage anisotropy, a value of zero indicates the elastic isotropy and a value of 100% identifies the largest possible anisotropy. The high-pressure dependences of the percentage anisotropy in compressibility and shear are tabulated in Table II. It is found that A_B and A_G have a trend of gradual decline as the pressure increases at first and turn to rise when the pressure increases continually.

The anisotropy of the crystal is also measured by A_+ and A_- coefficients calculated for every symmetry plane and axis. These factors are derived from elastic constants [51]. The calculated anisotropy factors of MgSiO₃ perovskite are presented in Table III. One can note systematic decrease in anisotropy factors of the crystal except symmetry plane (001) with increasing pressure.

IV. CONCLUSION

The thermodynamic and elastic properties of MgSiO₃ perovskite at different pressures and temperatures are investigated using the first-principles method based on the DFT and the quasi-harmonic Debye model. Through calculations, it is found that the calculated thermodynamic data are in good agreement with the available experimental data and the previous calculations. The thermal expansion coefficient and constant volume heat capacity are shown to converge to a nearly constant value at high pressures and temperatures. The elastic constants are predicted by using the finite strain method. From the elastic constants, using Hill's approximation, the ideal polycrystalline aggregates bulk modulus, shear modulus, Young's modulus, Poisson's ratio, and Debye temperature are calculated. Moreover, the bulk moduli along the crystallographic axes are also obtained.

V. ACKNOWLEDGMENTS

This work was supported by the National Natural Science Foundation of China (No.11064007 and No.11164013), the Natural Science Foundation of Gansu Province of China (No.1014RJZA046), the Program for New Century Excellent Talents in University, and the Key Project of Chinese Ministry of Education (No.209127).

- [1] H. K. Mao, R. J. Hemley, Y. Fei, J. F. Shu, L. C. Chen, A. P. Jephcoat, and Y. Wu, *J. Geophys. Res.* **96**, 8069 (1991).
- [2] L. Stixrude, R. J. Hemley, Y. Fei, and H. K. Mao, *Science* **257**, 1099 (1992).
- [3] T. Yagi and N. Funamori, *Philos. Trans. R. Soc. Lond. Ser. A* **354**, 1371 (1996).
- [4] I. Jackson, *Geophys. J. Int.* **134**, 291 (1998).
- [5] A. Yeganeh-Haeri, *Phys. Earth Planet. Inter.* **87**, 111 (1994).
- [6] A. R. Oganov, J. P. Brodholt, and G. D. Price, *Nature* **411**, 934 (2001).
- [7] A. R. Oganov, J. P. Brodholt, and G. D. Price, *Earth Planet. Sci. Lett.* **184**, 555 (2001).
- [8] B. B. Karki, L. Stixrude, S. J. Clark, M. C. Warren, G. J. Ackland, and J. Crain, *Am. Mineral.* **82**, 635 (1997).
- [9] R. M. Wentzcovitch, B. B. Karki, S. Karato, and C. R. S. da Silva, *Earth Planet. Sci. Lett.* **164**, 371 (1998).
- [10] F. C. Marton and R. E. Cohen, *Phys. Earth Planet. Inter.* **134**, 239 (2002).
- [11] R. M. Wentzcovitch, B. B. Karki, M. Cococcioni, and S. de Gironcoli, *Phys. Rev. Lett.* **92**, 018501 (2004).
- [12] E. Knittle and R. Jeanloz, *Science* **235**, 668 (1987).
- [13] G. Fiquet, A. Dewaele, D. Andrault, M. Kunz, and T. L. Bihan, *Geophys. Res. Lett.* **27**, 21 (2000).
- [14] E. Knittle and R. Jeanloz, *Nature* **319**, 214 (1986).
- [15] Y. Wang, D. J. Weidner, R. C. Liebermann, and Y. Zhao, *J. Geophys. Res.* **101**, 8257 (1994).
- [16] N. L. Ross and R. M. Hazen, *Phys. Chem. Miner.* **16**, 415 (1989).
- [17] B. B. Karki, R. M. Wentzcovitch, S. de Gironcoli, and S. Baroni, *Phys. Rev. B* **62**, 14750 (2001).
- [18] O. L. Anderson, *Am. Mineral.* **83**, 23 (1998).
- [19] Z. J. Liu, X. W. Sun, Q. F. Chen, L. C. Cai, H. Y. Wu, and S. H. Ge, *J. Phys.: Condens. Matter* **19**, 246103 (2007).
- [20] W. Kohn and L. J. Sham, *Phys. Rev.* **140**, A1133 (1965).
- [21] P. Hohenberg and W. Kohn, *Phys. Rev.* **136**, B864 (1964).
- [22] M. D. Segall, P. J. D. Lindan, M. J. Probert, C. J. Pickard, P. J. Hasnip, S. J. Clark, and M. C. Payne, *J. Phys.: Condens. Matter* **14**, 2717 (2002).
- [23] J. P. Perdew, K. Burke, and M. Ernzerhof, *Phys. Rev. Lett.* **77**, 3865 (1996).
- [24] H. J. Monkhorst and J. D. Pack, *Phys. Rev. B* **13**, 5188 (1976).
- [25] P. D'Arco, G. Sandrone, R. Dovesi, E. Apra, and V. R. Saunders, *Phys. Chem. Miner.* **21**, 285 (1994).
- [26] R. M. Wentzcovitch, N. L. Ross, and G. D. Price, *Phys. Earth Planet. Inter.* **90**, 101 (1995).
- [27] F. Birch, *J. Geophys. Res.* **83**, 1257 (1978).
- [28] S. K. Saxena, L. S. Dubrovinsky, F. Tutti, and T. L. Bihan, *Am. Mineral.* **84**, 226 (1999).
- [29] N. Funamori, T. Yagi, W. Utsumi, T. Kondo, and T. Uchida, *J. Geophys. Res.* **101**, 8257 (1996).
- [30] T. Tsuchiya, J. Tsuchiya, K. Umamoto, and R. M. Wentzcovitch, *Earth Planet. Sci. Lett.* **224**, 241 (2004).
- [31] M. A. Blanco, E. Francisco, and V. Luaña, *Comput. Phys. Commun.* **158**, 57 (2004).
- [32] X. W. Sun, Z. Y. Zeng, T. Song, Z. J. Fu, B. Kong, and

- Q. F. Chen, Chem. Phys. Lett. **496**, 64 (2010).
- [33] X. W. Sun, Q. F. Chen, X. R. Chen, L. C. Cai, and F. Q. Jing, J. Solid State Chem. **184**, 427 (2011).
- [34] T. S. Duffy and D. L. Anderson, J. Geophys. Res. **94**, 1895 (1989).
- [35] M. Akaogi and E. Ito, Geophys. Res. Lett. **20**, 105 (1993).
- [36] S. H. Shim, R. Jeanloz, and T. S. Duffy, Geophys. Res. Lett. **29**, 2166 (2002).
- [37] X. W. Sun, Z. J. Liu, Q. F. Chen, T. Song, and C. W. Wang, Chin. Phys. B **18**, 5001 (2009).
- [38] J. F. Nye, *Physical Properties of Crystals*, Ely House, London: Oxford University Press, (1957).
- [39] N. W. Ashcroft and N. D. Mermin, *Solid State Physics*, Orlando, FL: Harcourt Brace College Publishers, (1976).
- [40] F. I. Fedorov, *Theory of Elastic Waves in Crystals*, New York: Plenum Press, (1968).
- [41] W. Voigt, *Lehrbuch de Kristallphysik*, Leipzig: Terubner, (1928).
- [42] A. Reuss and Z. Angew. Math. Mech. **9**, 49 (1929).
- [43] R. Hill, Proc. Phys. Soc. London **65A**, 349 (1952).
- [44] A. Yeganeh-Haeri, D. J. Weidner, and E. Ito, in *Perovskite: a Structure of Great Interest for Geophysics and Materials Science*, A. Navrotsky and J. J. Weidner, Ed., Washington, DC: American Geophysical Union, (1989).
- [45] W. Köster and H. Franz, Metall. Rev. **6**, 1 (1961).
- [46] S. F. Pugh, Philos. Mag. **45**, 823 (1954).
- [47] O. L. Anderson, J. Phys. Chem. Solids **24**, 909 (1963).
- [48] E. Screiber, O. L. Anderson, and N. Soga, *Elastic Constants and Their Measurement*, New York: McGraw-Hill, (1973).
- [49] P. Ravindran, L. Fast, P. A. Korzhavyi, B. Johansson, J. Wills, and O. Eriksson, J. Appl. Phys. **84**, 4891 (1998).
- [50] D. H. Chung and W. R. Buessem, J. Appl. Phys. **38**, 2010 (1967).
- [51] K. Lau and A. K. McCurdy, Phys. Rev. B **58**, 8980 (1998).